Paper

Precise Speed and Torque Control for AC Traction Pure Electric Braking System in Low Speed Range

Student Member Lilit Kovudhikulrungsri (The University of Tokyo)
Member Takafumi Koseki (The University of Tokyo)

This paper describes a possibility to increase the operation range of railway's pure electric braking system at low speed range. Since low-resolution speed encoders are normally installed, precise speed information is unavailable at low speed. An estimation scheme called instantaneous speed observer is introduced to estimate the speed for precise torque and speed controls. The stability of the system is analyzed by multirate sampling theory and digital control theory. Several simulation results and experiments positively show the improvement of speed estimation and the possibility to extend the operation of the pure electric brake.

Keywords : Pure electric brakes, induction motors, low-resolution encoders, low speed, instantaneous speed observer, stability.

1. Introduction

The combination of air brakes and electric brakes plays a major role in braking systems of electric railway vehicles. This combination, however, often causes severe riding comfort and inaccuracy of stop position because of the slow response of the brakes' mechanical parts. Moreover, the physical characteristics of the mechanical parts, *i.e.* brake shoes, always vary with velocity, temperature and surface conditions.

To eliminate these problems, it is necessary to operate the electric brakes as the main braking scheme. This leads to the proposal of pure electric brakes[1]. The pure electric brakes can improve regenerative energy and riding comfort, since the response of the electric system is faster. If we can control the stop position precisely, the train automatic stopping control (TASC) can be realized.

One of the difficulties in realization is the precision of the speed information, which is necessary for a closed loop control. Since encoders installed in a vehicle have only 60 pulses per revolution (ppr), it is difficult to obtain speed information at every sampling time, especially at low speed. This results in the failure of the closed loop control. Consequently, the open loop control is applied when the vehicle speed drops below 5 km/h and a friction brake is normally applied. There are normally some shocks due to the transition of the switching of braking scheme and variation of braking force due to the manual operation. This finally results in a severe riding comfort. The use of the friction dependent mechanical brake also, moreover, deteriorates the accuracy of stopping position.

The dynamics of the railway vehicles is relatively simple, compared to robotics or other industrial drives although its drive technique cannot always be simple because there are some low frequency mechanical resonances in bogie systems. Especially, motor control for traction is straightforward since torque control is implemented. The vector control has been recently introduced to the vehicle. If some speed estimation scheme are applied, it is possible to achieve an effective motor drive or braking control.

Regarding to the problem of encoders, the application of speed sensorless drive techniques to traction are being studied . However, the speed estimation at low speed is difficult to achieve due to parameter variations.

Due to the existence of the speed encoders and the difficulties of the sensorless drive techniques, in this paper, we introduce an instantaneous speed observer, which can estimate the speed at every sampling when the speed signal from the encoder is not directly useful[2]. Since this paper deals with operation at low speed, the stability of the system is analyzed by multirate sampling and digital control theory. The proposed control system is verified through several simulations and experiments.

2. Instantaneous speed observer

In order to estimate the speed when the information from the encoder is unable to obtain frequently, an instantaneous speed observer is introduced to the system. Its timing diagram is shown in Fig. 1. The sampling instant [m,k] is defined by

$$t = T_1\left(\theta[m]\right) + kT_2 \equiv [m,k], \quad \cdots\cdots (1)$$

where T_1 and T_2 are the variable period between the encoder pulses and DSP (digital signal processor) sampling period, respectively.

By this definition, it is possible to estimate the rotor speed at any sampling instant $[m, k]$, starting from its value estimated in the previous sampling instant $[m, k\text{-}1]$, if we know the values of the produced torque, T_{em} and the mechanical disturbance torque, T_L

$$\hat{\omega}[m,k] = \hat{\omega}[m,k-1] + \frac{T_2}{2}\left\{\frac{T_{em}[m,k] + T_L[m] + T_{em}[m,k-1] + T_L[m]}{J}\right\}, \quad \cdots\cdots (2)$$

where J is the moment of inertia, ^ means estimated value and the definition of the symbols is given in Fig.2. The error of estimation is caused by two factors - the deviation of position detection from the encoder, $\Delta\theta$, and the disturbance torque,

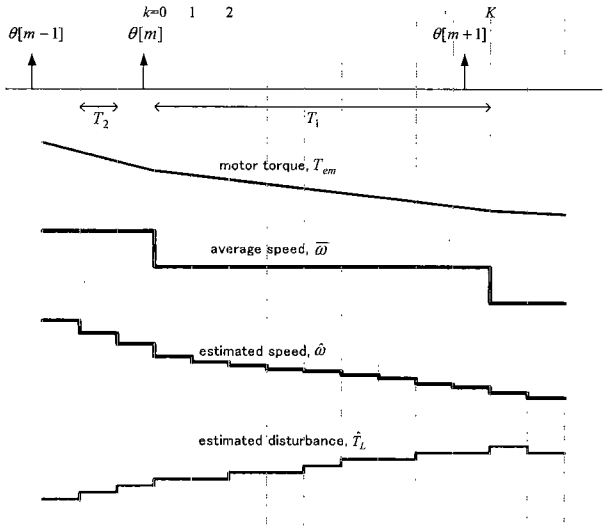

Fig. 1. Timing diagram of an instantaneaous speed observer.

ΔT_L. Hence, the update laws have been proposed by

$$\Delta\hat{\omega}[m+1] = \frac{\gamma_1 \Delta\theta[m+1]}{T_1}, \quad \cdots\cdots (3)$$

$$\Delta T_L[m+1] = \frac{2J\gamma_2 \Delta\theta[m+1]}{T_1^2}. \quad \cdots\cdots (4)$$

The coefficient γ_1 and γ_2 allow us to assign the desired estimation error dynamics. The observer is rearranged into state space variable

$$\hat{\mathrm{x}}[m+1] = \mathrm{A}\hat{\mathrm{x}}[m] + \mathrm{B}\mathrm{u}[m], \quad \cdots\cdots (5)$$

where

$$\hat{\mathrm{x}}[m] = [\hat{\omega} \quad \hat{T}_L]^T, \mathrm{u}[m] = [T_{em} \quad \varpi]^T,$$

$$\mathrm{A} = \begin{pmatrix} 1-\gamma_1-\gamma_2 & (1-\gamma_1-\gamma_2)\dfrac{T_1}{2J} \\ \dfrac{-2J\gamma_2}{T_1} & 1-\gamma_2 \end{pmatrix},$$

$$\mathrm{B} = \begin{pmatrix} (2-\gamma_1-2\gamma_2)\dfrac{T_1}{2J} & \gamma_1+2\gamma_2 \\ -\gamma_2 & \dfrac{2J\gamma_2}{T_1} \end{pmatrix}. \quad \cdots\cdots (6)$$

Note that ϖ is the average speed calculated from the encoder pulses.

Poles of the observer are identical to the eigenvalue of matrix **A**:

$$z^2 + (\gamma_1 + 3\gamma_2 - 2)z - \gamma_1 - \gamma_2 + 1 = 0. \quad \cdots\cdots (7)$$

3. Proposed control system

Fig. 2 shows the block diagram of the proposed control system. In order to obtain the fast dynamics, vector control strategy is applied to the traction motor. The current and speed controllers are designed based on coefficeint coordinationin characteristic polynomial[3]. The instantaneous

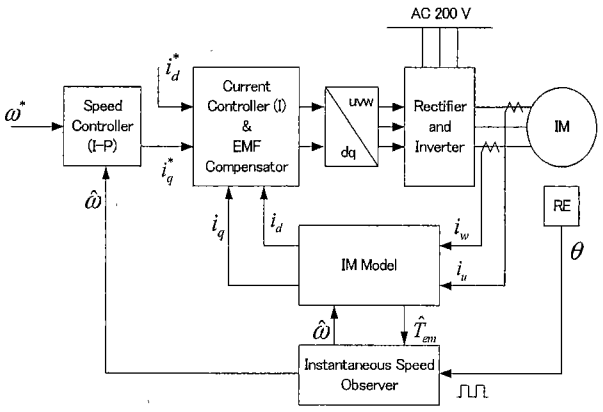

Fig. 2. The proposed control system.

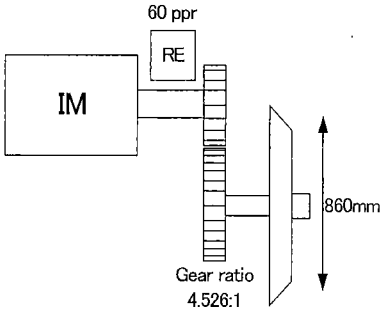

Fig. 3. Simplified drive system.

speed observer is introduced to the system to improve the speed information.

The desired dynamics of the instantaneous speed observer is obtained by assigning the location of the poles according to (7). In order to obtain the desired time response, the poles of the observer are placed on s-plane by the relation

$$s = \frac{\ln z}{T_1}. \quad \cdots\cdots (8)$$

Assuming that the observer poles on s-plane are located at $p\angle\phi$ and $p\angle-\phi$, we can correct the estimation error by the following equations[4],

$$\gamma_1 = \frac{1}{2} - \frac{3}{2}e^{2T_1 p\cos\phi} + e^{T_1 p\cos\phi}\cos(T_1 p\cos\phi), \quad \cdots\cdots (9)$$

$$\gamma_2 = \frac{1}{2} + \frac{1}{2}e^{2T_1 p\cos\phi} - e^{T_1 p\cos\phi}\cos(T_1 p\cos\phi). \quad \cdots\cdots (10)$$

The model of simulation, which is a simplified vehicle drive system is shown in Fig. 3. Note that the motor speed of 1 rpm corresponds to the vehicle speed of 1cm/s or 0.04 km/h. The motor parameters are listed in Table 1. The poles of control system on s-plane are found at. $6.97\angle\pm151^\circ$. Therefore, the observer poles are placed at $21\angle180^\circ$ on *s*-plane. The DSP sampling time, T_2, is set to 0.1 ms. Fig. 4 shows the simulation result. It is obviously seen that the estimated speed converges to the command. After 6 seconds, a braking command is introduced to the system and the speed drops. The estimated speed starts to oscillate at low speed range.

4. Stability Analysis

In the previous section, the validity of the application of the instantaneous speed observer has been examined. It was found that the system oscillated at low speed. In order to extend the operation range of the electric brake, it is necessary to analyze the stability of the observer. Since the observer estimates the value of the speed between the pulses at every sampling time of the DSP clock, it deals with two sampling times. One is the constant DSP clock sampling time. The other is the period between the pulses, which always varies, especially in braking operation. From this reason, the observer has been analyzed based on multirate sampling theory[5].

Fig. 5 shows the block diagram of the observer. Note that the observer is modified to full-order for simplicity in analysis and to see the behavior of the estimated position that will be used for error correction. The gain matrices and the variable vectors are described by

$$A_c=\begin{pmatrix}0&0&\frac{1}{J}\\1&0&0\\0&0&0\end{pmatrix},B_c=\begin{pmatrix}\frac{1}{J}\\0\\0\end{pmatrix},C_c=\begin{pmatrix}0\\1\\0\end{pmatrix},K=\begin{pmatrix}k_1\\k_2\\k_3\end{pmatrix},$$

$$u_c=T_{em},\ x_c=(\omega\ \theta\ T_L)^T \text{ and } y_c=\theta \quad \cdots\cdots (11)$$

The state equation of the observer is rearranged so that it is written in the from of

$$\dot{x}=Ax+Bu \quad \cdots\cdots (12)$$

Where

$$A=\begin{pmatrix}0&-k_1&\frac{1}{J}\\1&-k_2&0\\0&-k_3&0\end{pmatrix},B=\begin{pmatrix}k_1&\frac{1}{J}\\k_2&0\\k_3&0\end{pmatrix},$$

$$u=(\theta\ T_{em}) \text{ and } x=(\hat{\omega}\ \hat{\theta}\ \hat{T}_L)^T \quad \cdots\cdots (13)$$

The system is converted to discrete-time domain by the multirate sampling theory. Fig. 6 shows the expanded discrete-time signals. The produced torque, T_{em}, is read and the speed when the speed is estimated at every DSP sampling time, T_2, whereas the motor position is corrected when the next pulse is detected at the sampling time T_1. This T_1 is also defined as the sampling frame.

The pole placement is analyzed by using multirate sampling theory. It is found that the last sampling instants of each sampling frame contain enough information to detemine the behavior of the system [6]. We can adjust the dynamics of the observer by tuning the observer gains by the following equations,

$$k_1=\frac{(1-p_1)(1-p_2)+(1-p_2)(1-p_3)+(1-p_3)(1-p_1)}{T_1^2}, \quad \cdots\cdots (14)$$

$$k_2=\frac{(1-p_1)+(1-p_2)+(1-p_3)}{T_1}, \quad \cdots\cdots (15)$$

Table 1. Motor rating at 50 Hz and parameters.

rated voltage	100 V
rated current	13.6 A
rated power	1.5 kW
rated speed	1420 rpm
number of poles	4
Stator resistance	1.54 Ω
Rotor resistance	1 Ω
Stator leakage inductance	6.6 mH
Rotor leakage inductance	1.55 mH
Magnetizing inductance	111 mH

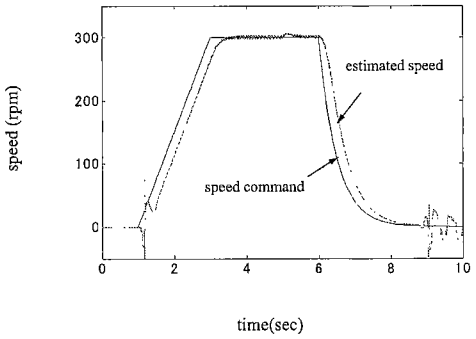

Fig. 4. Simulation result.

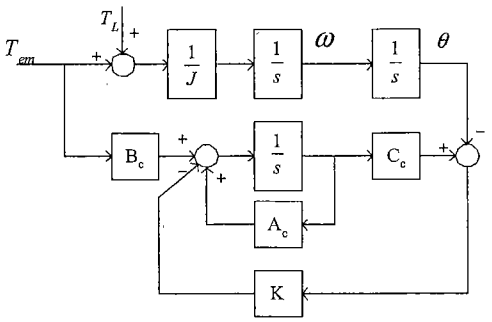

Fig. 5. Block diagram of a speed observer.

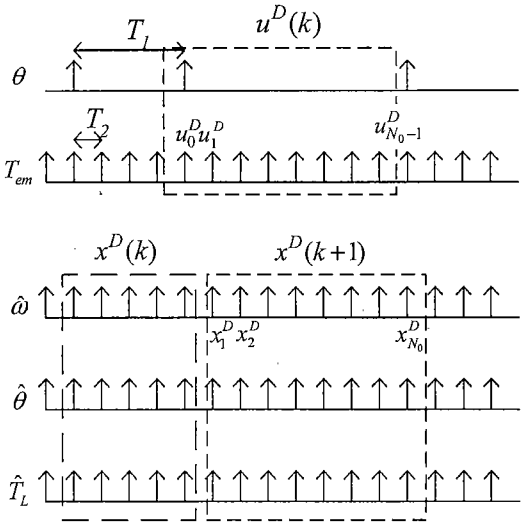

Fig. 6. Expanded discreted-time signals.

$$k_3 = J\frac{(1-p_1)(1-p_2)(1-p_3)}{T_1^3}, \quad \cdots\cdots (16)$$

where p1,p2 and p3 are poles of the observer on s-plane.

Fig. 7 and 8 shows the estimated speed when the speed commands are fixed at 300 rpm and 5 rpm, respectively. The observer poles are placed at $210\angle 180°$ on s-plane. There is no relative oscillation at 300 rpm but the oscillation occurs within a constant band of 2 rpm at 5 rpm.

To improve the stability and the performance of the observer, it is necessary to consider the relationship between the Nyquist frequency and the locations of the poles. The Nyquist angular frequency is found from

$$\Omega = \frac{\pi}{T_1}. \quad \cdots\cdots (17)$$

Fig. 9 shows the poles on z-plane according to the cases in Fig. 7 (300 rpm) and Fig. 8 (5 rpm). The pole locations in case of 300 rpm are illustrated by the right cross, while the other case is indicated by the left one. It is obviously seen that when speed drops, the poles move toward outside of the "effective region", where the natural frequency, ω_n, is less than the Nyquist frequency, Ω (the shaded area, i.e., the natural frequency is greater than the Nyquist frequency). This results in oscillation as shown in Fig. 8.

To improve the stability of the system, it is necessary to place the poles inside the effective region. For assurance of the stability without harmful oscillation of high frequency, we constrain so that the poles are placed inside 50 percents of the Nyquist frequency and the damping ratio of 0.5. We define this region as "conservative region" in this paper. This, however, slows down the response of the system. To obtain a faster response, the location of the poles can be placed at a smaller value of damping factor. Fig. 10 shows the new pole locations according to damping ratio of 0.7 and 20 percents of the Nyquist frequency. Note that region enclosed by the inner contour corresponds to 50 percents of the Nyquist frequency and the damping ratio of 0.5. The simulation according to the new pole locations is shown in Fig. 11. The oscillation has been effectively removed. We can conclude that at low speed, the observer pole on s-plane should be placed so that they always locates within the conservative region, i.e., the poles are fixed on z-plane.

Since fixing the observer poles on z-plane results in slow down of the observer dynamics, it is necessary to reduce the controller gains so that the observer response remains faster. The pole assignment strategy is summarized in Table 2.

The simulation result is shown in Fig. 12. After the braking command is input, the speed drops and the location of the observer pole on z-plane change until it reaches the critical speed. The observer poles on z-plane are then fixed and the controller gains are reduced, resulting in the slower but stabler

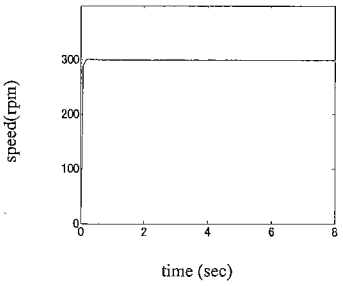

Fig. 7. Simulation result at the command of 300 rpm.

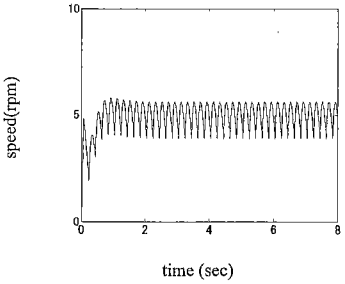

Fig. 8. Simulation result at the command of 5 rpm.

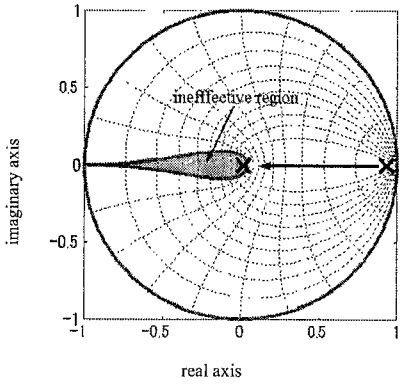

Fig. 9. Movement of poles when speed drops.

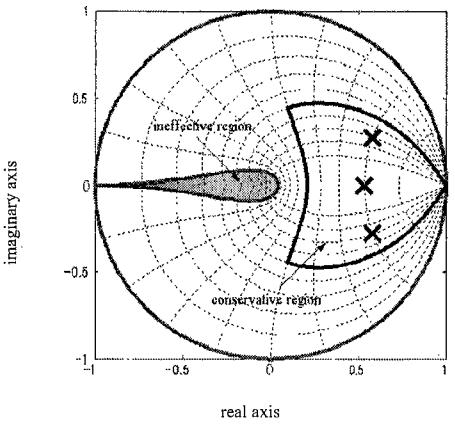

Fig. 10. New pole locations at the command of 5 rpm.

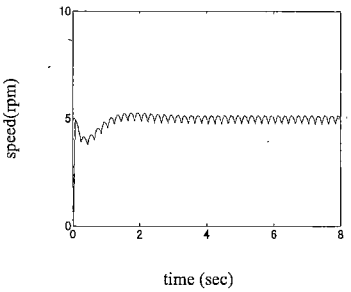

Fig. 11. Simulation result at the command of 5 rpm due to the new pole location.

response. Due to the simulation result, it can be the vehicle speed of 0.04 km/h. At this point, the vehicle operated close to the motor speed of 1 rpm, corresponding to can be stopped by locking the wheels without ware and tear of mechanical components.

Table 2. Pole assignment strategy.

Rotational speed	High	Low
Observer poles	fix on s-plane	fix on z-plane
system poles	fix on s-plane	fix on z-plane

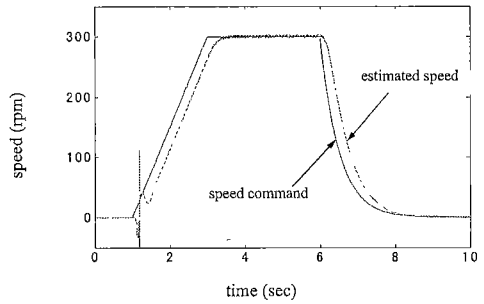

Fig. 12. Simulation result due to the new pole locations.

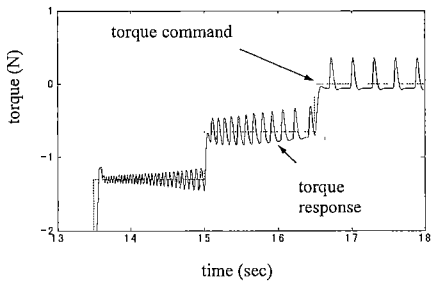

(a) Torque response without observer

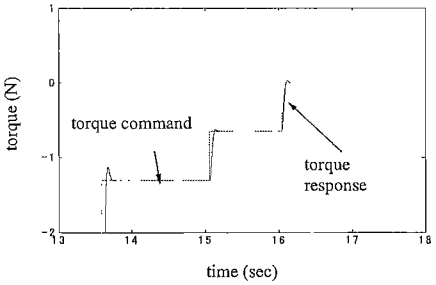

(b) Torque response with observer

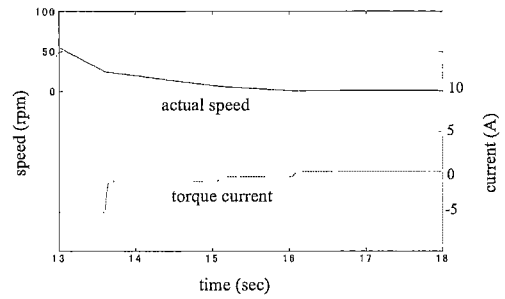

(c) Actual speed according to the torque current

Fig. 13. Simulation results of torque contro.

5. Simulation results according to torque or current command

In the present traction control, the acceleration and braking operations are achieved by notch commands, which are the levels of the torque-producing current. The appropriate notch commands are determined by the driver. Only the current, i.e., torque control loops are enough for manual operation since the driver acts as a speed controller. Precise speed information is, however, still necessary in manual operation since it is used for vector rotation. Fig. 13(a) and (b) show the torque response without and with the observer, respectively. Note that the pole assignment strategy in Table 2 is implemented. It is found that the torque response without the observer oscillates at low speed. As a result the electric braking cannot be implemented. On the other hand, the torque response with the observer has less oscillation. Fig. 13(c) shows the simulation results due to the torque response in Fig. 13(b). It is obviously seen that the oscillation does not occur at low speed and the proposed system gives much better braking force response also in the present manual speed control than a conventional system.

6. Experimental Results

Various experiments have been carried out to examine the validity of applying the observer to the system. The apparatus

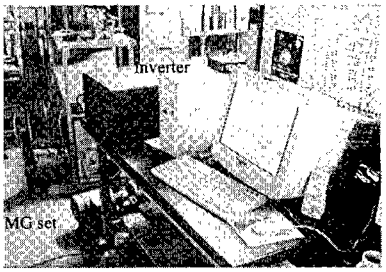

(a) MG set, inverter and controlling PC

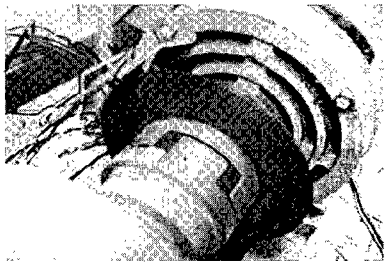

(b) Encoder

Fig. 14. Experimental apparatus.

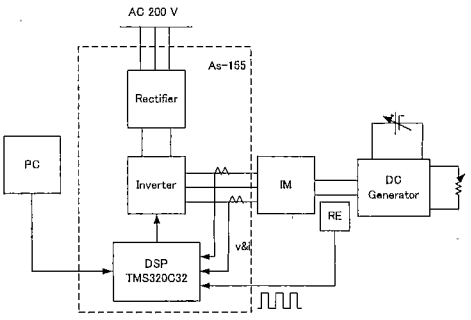

Fig. 15. Experiment setup.

and the experiment setup are shown in Fig. 14 and 15, respectively.

Since the DC generator is used as a load, the mechanical load becomes zero at low speed. This does not correspond to real traction, where the moment of inertia is much larger and effect of slope exists.

Even though the experiment at low speed cannot be realized for this reason, the operating condition of the observer at low speed can be tested by reducing the resolution of the encoder so that the corresponding interval between the pulses can be obtained. For instance, if we want to examine the operation at 10 rpm by a 60-ppr encoder, we must reduce the resolution to 6 ppr and operate the motor at 100 rpm. For this condition, the period between the pulse is 0.1 s, the observer time constant is fixed at 0.09 s and the speed controller equivalent time is fixed at 0.09 s and the speed controller equivalent time constant is 1.68 s.

Fig. 16 and 17 show the speeds calculated directly from a 6-ppr encoder and the estimated speed from the observer,

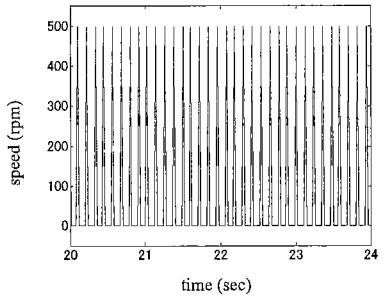

Fig. 16. Speed calculated directly from the encoder when the pulse interval is 0.1 second (equivalent to the pulse condition of a 60-ppr encoder when the motor rotate at 10 rpm).

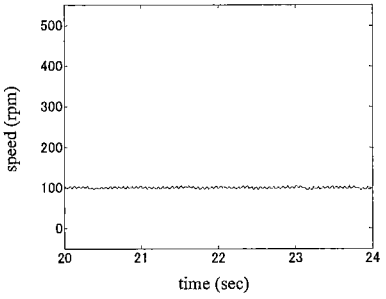

Fig. 17. Speed estimated from the observer when the pulse interval is 0.1 second.

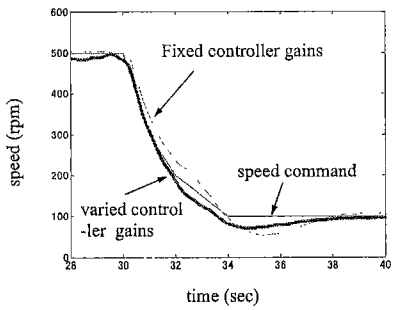

Fig. 18. Response when Speed drops when the pulse interval is 0.1 second.

respectively, when the motor runs at 100 rpm. It is obviously seen that the application of the observer improves the speed information. This also confirms that the observer works effectively even at the condition where the encoder pulses cannot be detected frequently

The experimental results when the reference speed gradually drops are shown in Fig. 18. The speed overshoot, which will be fatal in real braking operation, can be suppressed by by reducing the controller gain as summarized in Table 2.

7. Conclusions

This paper has proposed to introduce an instantaneous speed observer to improve the speed information especially at low speed. Since the observer can estimate the speed at every sampling time of the DSP, the precise speed control can be realized. The stability analysis based on multirate sampling theory and digital control theory has been carried out and it leaded to the conclusion that fixing the observer poles on z-plane can improve the stability at low speed. The simulation result showed the possibility to extend the electric brake until pulses. The application of the instantaneous speed observer to AC traction system will be an effective technique solution for condition where the encoder pulses cannot be detected encoder the motor speed of 1 rpm or 0.04 km/h, corresponding to the vehicle speed. The validity of the observer in critical realizing pure electric ordinary braking of electric railway vehicles.

(Manuscript received Jan. 21,2002, revised June 12,2002)

References

(1) S. Sone : "Power Electronic Technologies for Low Cost and Energy Conservation on World Railways Vehicles", Proc. IPEC-Tokyo2000, vol.1, pp. 452-457 (2000)

(2) Y. Hori : "Robust Motion Control Based on a Two-Degrees of-Freedom Servosystem", *Advanced Robotics*, vol 7, No.6, pp.525-546 (1993-6)

(3) Y. Hori, and K. Ohnishi : *Applied Control Engineering*, pp.135-137, Maruzen

(4) L. Kovudhikulrungsri and T. Koseki : "Speed Estimation of Induction Motor in Low Speed for Pure Electric Brake", Transportation, *Electric Railways and Linear Drive Conf.*, pp.19-24, Sapporo, July (2000)

(5) M. Araki, and K.Yamamoto, "Multivariable Multirate Sam-pled-Data System : State-Space Description, Transfer Characteristics and Nyquist Criterion" *IEEE Trans. Automatic Control*, vol. AC-31, pp.145-154 (1986)

(6) L. Kovudhikulrungsri, and T Koseki : "Stability Analysis of an Instantaneous Speed Observer for an Induction Motor with a Low-Resolution Encoder", *J-RAIL 2000*, Kawasaki, Dec., (2000)

Lilit Kovudhikulrungsri (Student Member) was born in Bangkok, Thailand on the 17th September 1977. He received a master degree in electrical engineering from the University of Tokyo in 2001 and is presently a Ph.D. student in the same university.

His research fields are electric drives, control system and railway engineering.

Takafumi Koseki (Member) was born in Tokyo on the 29th July 1963. He received a Ph.D. degree in electrical engineering from the University of Tokyo in 1992 and is presently an associate professor at the Department of Information and Communication, the University of Tokyo. He is studying applications of electrical engineering to public transport system, especially, to linear drives, and analysis and control of traction system.